Pergamon

Int. J. Heat Mass Transfer. Vol. 41, No. 11, pp. 1573–1584, 1998

Printed in Great Britain
0017-9310/98 $19.00+0.00

PII: S0017-9310(97)00203-2

Application of wide band radiation models to non-homogeneous combustion systems

P. S. CUMBER,† M. FAIRWEATHER and H. S. LEDIN

BG Technology, Research and Technology, Gas Research and Technology Centre, Ashby Road, Loughborough, Leicestershire LE11 3GR, U.K.

(*Received* 9 *September* 1996 *and in final form* 27 *June* 1997)

Abstract—A spectral version of the exponential wide band model has been adapted for implementation within a computational fluid dynamic framework. The model has been assessed by comparing predicted spectral and integrated quantities with experimental data and statistical narrow band model results for a number of idealised homogeneous and non-homogeneous configurations, and for a jet flame. Overall, the spectral wide band approach has been shown to be in reasonable agreement with experimental data, and to have an accuracy, for total quantities, comparable to that of the narrow band model whilst requiring almost an order of magnitude less computer processor time. © 1998 BG plc. Published by Elsevier Science Ltd. All rights reserved.

1. INTRODUCTION

There are many combustion applications where it is important to be able to model accurately radiative heat loss combined with other modes of heat transfer and fluid flow. Examples include fires in enclosures, and in particular the prediction of flash-over and flame spread, as well as assessments of the safety of gas venting and flaring operations. Another application where accurate modelling is particularly important is in the design of burners and furnaces, where a primary objective is the minimisation of emissions of oxides of nitrogen, since NO_x production is highly sensitive to local flame temperatures.

Modelling thermal radiation in conjunction with solutions of the fluid dynamic equations for a combusting system is a difficult task. In some situations, however, the influence of radiative heat transfer on fluid motion is small, with heat loss only causing small perturbations to the density field of the combusting flow. In such cases radiative heat transfer can be modelled using relatively crude approaches as, for example, when heat loss is introduced directly into laminar flamelet prescriptions used as the basis of the combusting flow calculations [1]. The fluid dynamic system of equations can then be converged in an uncoupled fashion without the explicit need of any model of radiative transfer, although the radiation incident on any surface of interest can be calculated subsequently using more sophisticated approaches [1]. For other areas of application, such as those noted above, radiative heat transfer has a sufficiently large effect on the flow field to require accurate calculation of heat transfer and fluid flow in a coupled manner.

There are two aspects of the radiative heat transfer process that require modelling: one is the transfer of radiant energy in the participating media, described by the radiative transfer equation, and the second is the adsorption, emission and scattering of radiation by the participating media itself. For the type of radiative transfer equation solution method considered later, the former problem reduces to one of describing the dependence of the intensity of radiation on the direction cosines that define a pencil of radiation. This is a geometric problem for which a number of methods of solution exist, examples being the discrete transfer [2] and discrete ordinate [3] methods. Both these techniques solve the transfer equation along a number of representative rays, with the accuracy of the solution obtained being simply a function of numerical error that can be reduced to any level required by solving for more rays or directions.

The modelling of participating media introduces a second form of error; namely the physical error implicit in the underlying assumptions of the model implemented. In reality, the significant computational cost associated with solving a system of transport equations makes it desirable to model such contributions to the heat transfer process as economically as possible. As a consequence, one option that is superficially attractive, as the computational overhead is small, is to specify a mean absorption coefficient based on a curve fit to total emissivity data for each control volume in the computational mesh used in solving the flow equations. The participating media is therefore assumed to be grey, and a non-homogeneous path is approximated as a sequence of homogeneous elements. The inputs to the curve fit to emissivity data are then local compositions and a length scale calculated from the dimensions of the control volume. For this approach to be valid, predicted radiation

† Author to whom correspondence should be addressed.

NOMENCLATURE

A	total band absorption
A_Q	numerical quadrature of equation (2)
C	constant
d	line spacing
f_v	soot volume fraction
I	radiant intensity
$I_{b,v}$	black body spectral intensity
I_λ, I_v	spectral intensity
K_a	grey gas absorption coefficient
K_v	spectral absorption coefficient
l	path length
P	total pressure
P_e	equivalent broadening pressure parameter
P_j	partial pressure of gaseous species j
q	radiative heat flux
r	radial distance
S	mean line intensity
T	temperature
x	axial distance
X	partial density path length.

Greek symbols

α	integrated band intensity
β	mean line width-to-spacing parameter
Δv	band width
η	line width-to-spacing ratio
λ	wave length
v	wave number
ρ	partial density
$\tau_{g,v}$	spectral transmittance of gas phase
τ_H	optical depth at band head
$\tau_{s,v}$	spectral transmittance of soot
$\tau_{\Delta v}$	band transmittance
τ_v	total spectral transmittance
ω	band width parameter.

Subscripts

i	gas band
j	gaseous species
$n, n-1$	exit and entry points of ray traversing control volume
u	upper
Δv	band quantity
v	spectral quantity.

intensities should converge as the representation of the non-homogeneous path is refined through the use of more homogeneous control volumes. In practice, however, this is not the case since as path length is reduced the mean absorption coefficient increase in dK_a/dl does not tend to zero. This in turn implies that as the computational mesh is refined the sensitivity of the predicted intensity field to local path length increases. This problem is well known in the radiation modelling community, but applications of this type of methodology, in conjunction with numerical solutions to the flow equations, still appear in the literature.

Edwards [4] coined the phrase "the grey gas myth", and demonstrated how a grey analysis for a molecular gas with banded emission has dubious utility. A model with a more subtle basis must therefore be used where emission from molecular gases is an important part of the heat transfer process. A number of models for participating media that can be used in conjunction with computational fluid dynamic solutions of the fluid flow equations exist in the literature, with the different models varying in their level of sophistication, generality, accuracy and computational cost. Examples include mixed grey gas models [5], the total transmittance non-homogeneous model [6], and exponential wide [7] and statistical narrow band models [6].

The present paper uses an extension of Edwards and Balakrishnan's [7] formulation of the exponential wide band model within a computational fluid dynamic framework. There are a number of features of this model that make its further investigation appealing: it has a sound physical basis [8]; has been shown to provide a reasonable fit to data obtained over a wide range of conditions [8–10]; and the computational cost of the model is typically an order of magnitude less than statistical narrow band approaches [11]. The wide band model can, of course, be applied directly to non-homogeneous systems using the technique of wide band scaling [4] which solves the radiative heat transfer equation in its integral form. The approach does not, however, easily lend itself to coupling with fluid dynamic calculations where the radiation intensity field throughout the computational domain is required in order to determine source terms for use in solving an energy transport equation. As a consequence, a number of authors have considered using the wide band model for predicting radiative heat transfer in non-homogeneous systems, without the need for wide band scaling [4]. Docherty and Fairweather [12] used the banded version of Edwards and Balakrishnan's [7] exponential wide band model in conjunction with an adaptation of the discrete transfer method. The overall model can be applied to combustion systems by approximating a non-homogeneous profile as a sequence of homogeneous elements and solving the radiative transfer equation by applying a suitable banded recurrence relation. This model was validated, through inclusion of Modak's [13] model for emissions from soot, by

comparison of predicted spectral and total intensities with results derived from a narrow band model for a number of non-homogeneous situations representative of various lines-of-sight through turbulent non-premixed flames. Agreement between the overall model and narrow band results was encouraging. However, application of the model, which uses the four-region approximate expression to calculate band absorptance discussed further below, is dependent on increasing the upper bound on band transmittance recommended by Edwards [4], subject to the proviso that the band transmittance still behaves as if grey at small optical depths.

Komornicki and Tomeczek [11] also modified Edwards and Balakrishnan's [7] exponential wide band model for application to flames, their motivation again being the upper bound on band transmittance used in the banded version of the original formulation. These authors noted that for small optical depths this version of Edwards and Balakrishnan's [7] model gave inaccuracies in band absorptivity, when compared to narrow band results, despite band absorption being predicted to an acceptable level. They therefore calculated absorptivities for those bands of importance in the combustion products of natural gas using a narrow band model, and tabulated these results in terms of temperature and partial pressure path length for a total pressure of one atmosphere. Data from the latter tables was subsequently used in specifying the band absorptivities required in the wide band model, with all other aspects of the model being the same as in the original [7] banded formulation. The model was validated by comparing total intensities predicted for two lines-of-sight through a 750 kW natural gas furnace flame with narrow band model results and experimental measurements, with good agreement being obtained. Unfortunately, Komornicki and Tomeczek only calculated band absorptivities for the major participating species, neglecting the 2.34 μm CO band, the 2.0, 9.4 and 10.4 μm CO_2 bands, and all CH_4 bands, which inevitably restricts the overall applicability of the model.

Although it is possible to extend Komornicki and Tomeczek's [11] modification to the wide band model to include these bands, the original spectral formulation [7] of the wide band model can be used within a fluid dynamic framework without restrictions imposed on its range of applicability. Use of the methodology described below also avoids the need to increase Edwards' [4] upper bound on band transmittance, required in the technique described by Docherty and Fairweather [12], which makes implementation within any computational fluid dynamic model cumbersome.

2. BASIS OF THE EXPONENTIAL WIDE BAND MODEL

The versions of the exponential wide band model considered in the present paper are based on the original formulation of Edwards and Balakrishnan [7], also described in detail by Edwards [4]. As the derivation of the model is lengthy, attention below is restricted to the salient points.

The model is based on the fact that the absorption and emission of infra-red radiation by a molecular gas is generally concentrated in between one and six wide bands which are associated with vibrational modes of energy storage by the molecule. Within these vibrational bands are a large number of spectral lines which are associated with rotational modes of energy storage. In the wide band model a detailed knowledge of the position and intensity of these rotational lines is considered to be unimportant, such that they can be re-ordered in wave number space with exponentially decreasing line intensities moving away from the band head. The band shape is then approximated by one of three simple exponential functions depending upon whether a lower limit, upper limit or band centre wave number is used to prescribe the position of the band head, and radiative properties are obtained by specifying three model parameters that characterise a given absorption band: an integrated band intensity, α, a mean line width-to-spacing parameter, β, and a band width parameter, ω. Values of all these variables have been evaluated by Edwards and Balakrishnan [7] for the bands of a number of molecular gases. For an asymmetric band with upper limit ν_u, the mean line intensity to spectral line spacing ratio is given by

$$S/d = (\alpha/\omega)e^{-(\nu_u-\nu)/\omega} \tag{1}$$

with band absorption being calculated from

$$A = \int_0^{\infty} \left(1-\exp\left[\frac{-(S/d)X}{(1+(S/d)X/\eta)^{1/2}}\right]\right)\mathrm{d}(\nu_u-\nu) \tag{2}$$

where $\eta = \beta P_e$. Similar expressions are used for bands specified by their lower limit or band centre. Edwards and Balakrishnan [7], and later Edwards [4], proposed that a four-region approximate expression be used to replace the above integral in hand calculations of band absorptance:

$$\begin{aligned} A/\omega &= \tau_H \quad \tau_H \leqslant 1, \tau_H \leqslant \eta \\ A/\omega &= (4\eta\tau_H)^{1/2} - \eta \quad \eta \leqslant \tau_H \leqslant 1/\eta, \eta \leqslant 1 \\ A/\omega &= \ln(\tau_H\eta) + 2 - \eta \quad 1/\eta \leqslant \tau_H \leqslant \infty, \eta \leqslant 1 \\ A/\omega &= \ln\tau_H + 1 \quad \tau_H \geqslant 1, \eta \geqslant 1 \end{aligned} \tag{3}$$

where τ_H is the optical depth at the band head. The transmittance of the band is then given by

$$\tau_{\Delta\nu} = (\tau_H/A)(\mathrm{d}A/\mathrm{d}\tau_H). \tag{4}$$

This is equivalent to assuming that absorption within a band is grey, and in the same way that the grey gas assumption can lead to problems, for small path lengths the grey band assumption also breaks down such that a lower limit on band absorptivity must be

imposed. Edwards [4] does this by imposing an upper bound on band transmittance:

$$\tau_{\Delta\nu} \leftarrow \min(\tau_{\Delta\nu}, 0.9). \tag{5}$$

Lastly, the width of the band is

$$\Delta\nu = A/(1-\tau_{\Delta\nu}) \tag{6}$$

and, given the position of the band head, both the upper and lower limits of the band in wave number space can be determined. A number of quantities have been introduced above with no further explanation or discussion. A full account of the model can be found in Edwards and Balakrishnan [7] and in Edwards [4].

The above analysis is for a single band. Where a gas with more than one band, or a mixture of gases, is present, a piece-wise constant approximation to the spectral transmittance can be calculated. This is done by applying the above procedure to each band and, where bands overlap in wave number space, the spectral transmittance is taken to be the product of the band transmittances.

As noted earlier, the version of the wide band model described above can lead to problems when used in conjunction with solutions of the radiative transport equation within fluid dynamic codes. In particular, its application together with the type of recurrence relation used in the discrete transfer method can result [11] in the predicted radiation intensity failing to converge as the number of homogeneous elements used to represent a non-homogeneous profile increases, i.e. as the number of control volumes used in any fluid dynamic calculation increases. This occurs because of the break down of the grey band assumption at small path lengths. This problem can be alleviated by increasing the upper limit on band transmittance imposed through equation (5), provided that $\tau_{\Delta\nu}$, still behaves as if grey as path length decreases, although the latter condition makes implementation within any computation fluid dynamic framework difficult. Alternatively, the approach of Komornicki and Tomeczek [11] can be used, with band absorptivities calculated using a narrow band model.

The present work employs an alternative approach, as originally used by Edwards and Balakrishnan [7]. The grey band assumption necessary in calculating the band absorptance using equation (3) is therefore avoided by employing the analytic expressions, equation (2) and its variants, to model band transmittance. The spectral transmittance for a mixture of gases is then taken to be

$$\tau_{g,\nu} = \exp\left(-\sum_{ij} \frac{(S/d)_i X_j}{[1+(S/d)_i(X/\eta)_j]^{1/2}}\right) \tag{7}$$

where i denotes a particular gas band and j a participating species. Specifying the spectral transmittance for participating gases using the above equation makes implementation within either the discrete transfer or discrete ordinate method straightforward, as the spectral absorption coefficient is given simply by

$$K_\nu = \sum_{ij} (S/d)_i \rho_j [1+(S/d)_i(X/\eta)_j]^{-1/2}. \tag{8}$$

Moreover, as the path length is reduced

$$K_\nu \to \sum_{ij} (S/d)_i \rho_j \tag{9}$$

so that the grid independent predictions can be obtained when this version of the exponential wide band model is applied to combusting flows within a computational fluid dynamic framework.

One problem does arise in using equation (2) and its variants directly, rather than equation (3), in spectral calculations. In deriving optimum values for the three model parameters that characterise a given absorption band, fits to experimental data for α, β and ω were obtained in conjunction with the four-part expression. Edwards and Balakrishnan [7] therefore recommended that in spectral calculations for homogeneous gases the ratio of band absorptions (A/A_Q) determined from equations (3) and (2), respectively, be derived, and values of α and ω multiplied by this ratio in order to achieve a similar level of agreement for total quantities as would be obtained using the four-part expression. Use of this correction in non-homogeneous calculations is, however, inappropriate [7], and complicated by the fact that A/A_Q is not a smooth function which in turn causes problems as increasing numbers of homogeneous cells are used to represent a non-homogeneous profile. Edwards [4] subsequently modified this recommendation, in line with Edwards and Balakrishnan's [7] suggestion for non-homogeneous systems, and proposed that adjusting ω alone upward by 20% was adequate for spectral calculations given that the data originally fitted using the four-part expression was only correlated to within 15%. A modified version of the latter approach was adopted in deriving the predictions given in the remainder of this paper. Thus, for small path lengths, where the linear relation of the four-part expression [equation (3)] is valid, it can be shown, by expanding equation (2) as a Taylor series in the partial density path length, that

$$A_Q = A + O(X^2). \tag{10}$$

Results were therefore derived by increasing ω by 20%, apart from in the region $\tau_H \leqslant \eta \leqslant 1$ where no correction was applied.

In the results given below, calculations for non-homogeneous paths were based on numerical solutions of the equation of radiative heat transfer obtained using a similar approach to that adopted by Docherty and Fairweather [12]. The exponential wide band model was therefore used to calculate the transmittance of participating gaseous species and, where required, soot transmittance was taken as

$$\tau_{s,\nu} = \exp(-Cf_v vl) \tag{11}$$

where C is a constant taken, from [5], to be 7.2. The spectral transmittance for a mixture of gaseous species and soot is then

$$\tau_\nu = \tau_{g,\nu}\tau_{s,\nu}. \quad (12)$$

Finally, the spectral intensity distribution was calculated by applying the recurrence relation

$$I_{n,\nu} = I_{n-1,\nu}\tau_\nu + I_{b,\nu}(1-\tau_\nu) \quad (13)$$

to the sequence of homogeneous volumes used to approximate a non-homogeneous path at a set of discrete points uniformly spaced in the region of wave number space of interest. Total intensities were then determined by numerically integrating the spectral intensity distribution using a composite trapezoidal quadrature rule [14]. It was found that 80 points over the wave number interval $10 < \nu < 10\,000$ were sufficient in predicting the radiation fields considered below. Doubling this number of points changed predictions by 5% at most.

3. MODEL EVALUATION

Before considering application of the method described to non-homogeneous calculations, it is useful to first compare predictions of the spectral technique with results derived from the banded formulation and with experimental data. The first configurations considered are three homogeneous paths of length 0.39 m, where the participating species are CH_4, CO_2 and H_2O. Measurements of spectral absorptivity with wave number are available [4] for these configurations, with details of the total and partial pressures, and temperatures, examined being given in Table 1. Figure 1 shows measured and predicted spectral absorptivities for these three situations, whilst Table 1 includes total integrated absorptivities. Comparing the performance of the two models, the spectral method is obviously superior from a qualitative point of view since the spectral absorptivity shown in Fig. 1 is a smooth function, compared to the piece-wise constant function used in the banded approach. Quantitatively, and with reference to the results of Fig. 1 and Table 1, the spectral method is marginally more accurate than the banded approach. Of the homogeneous paths considered, the poorest agreement with measurements is for CH_4 where both modelling

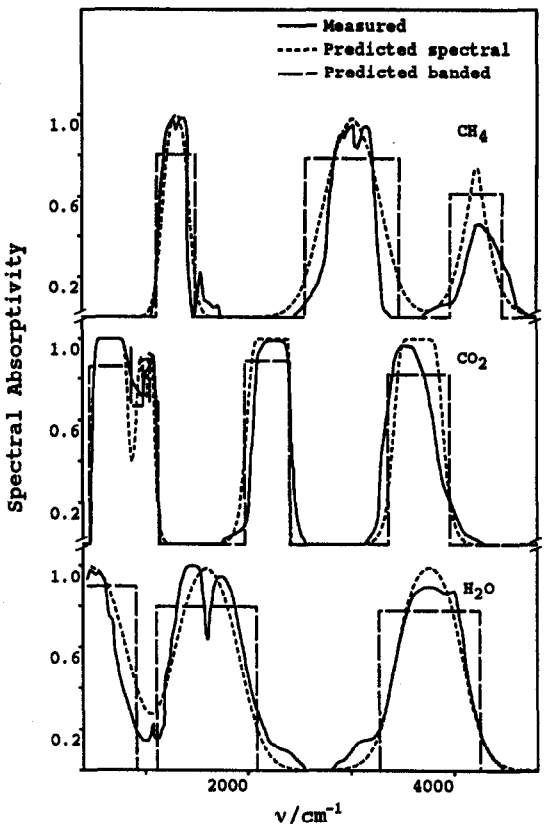

Fig. 1. Measured and predicted spectral absorptivities for three homogeneous paths.

approaches suffer from inaccuracies in the exponential tail representation of the 3.3 μm band [4]. Also included in Table 1 is a fourth case for which data is available, see Siegel and Howell [15]. This case is of interest as the wave number range examined includes the 2.0 μm band of CO_2 which is outside the range of the data given for the other three situations. As for the other cases considered, use of the spectral method again gives results in closer agreement with observations.

All these comparisons serve to confirm the superiority of the spectral over the banded method, although in some cases this is marginal in terms of total absorptivities. Edwards and Balakrishnan [7] performed

Table 1. Total absorptivities for four homogeneous paths

Gas	P [atm]	P_j [atm]	T [K]	Total absorptivity		
				Measured	Predicted banded	Predicted spectral
CH_4	3.20	0.80	833.00	0.21	0.28	0.25
CO_2	10.00	10.00	1389.00	0.23	0.22	0.23
H_2O	2.0	2.00	833.00	0.43	0.46	0.41
CO_2	10.00	10.00	833.00	0.29	0.26	0.28

similar calculations for various mixtures of CO_2 and H_2O at differing temperatures, and total and partial pressures, and found that both the spectral and banded methods were in general within 10% of observations, with the former method again being marginally in closer agreement with total emissivities and absorptivities derived from the data.

Turning to an evaluation of the spectral method for application to non-homogeneous paths, there is, in general, an absence of experimental data for radiation intensities in well-characterised combustion systems. As a consequence, the calculation method was validated by comparison with predictions of a statistical narrow band model [6, 16] for a number of idealised one-dimensional situations. The accuracy of the latter model for predicting both homogeneous and non-homogeneous systems is well documented [6, 16, 17]. Figure 2 shows temperature and partial pressure profiles for four non-homogeneous paths studied by Grosshandler [6]. Configuration *A* approximates the distributions that might be found parallel to the surface of a pool fire, whilst configurations *B* to *D* represent rearrangements of these base case distributions, or portions thereof. Predictions of right-directed radiation intensity for all four cases are given in Fig. 3, where results were derived for path lengths ranging from 0.05–1.0 m as additional elements of the temperature and partial pressure profiles were added to the line-of-sight. For all these configurations, spectral wide band model results were obtained using varying numbers of homogeneous cells to represent the non-homogeneous profiles. In general, predictions derived using 18 and 36 homogeneous cells were identical, with results obtained using nine cells being at variance from converged values by a maximum of 10%. It is converged values that are considered in Fig. 3, and in the remainder of the paper.

Results derived from the spectral wide band approach are seen to be in close agreement with narrow band predictions for all four configurations. Qualitatively, agreement between the two methods is good, with the spectral approach reproducing the location of minima and maxima in the narrow band results caused, respectively, by the addition of hot emitting or cold absorbing layers of gas to a line-of-sight. Quantitatively, the deviation between the two methods generally increases with path length, although the maximum error is only 12%.

Comparison of spectral intensities obtained from the two modelling approaches is made in Fig. 4. These results were derived for the profiles of configuration *A*, at a path length of 1 m, and for low ($f_v = 5.55 \times 10^{-8}$) and high ($f_v = 1.11 \times 10^{-6}$) soot loadings distributed uniformly across the total path length. In both cases, agreement between results derived from the two models is good. For the low soot

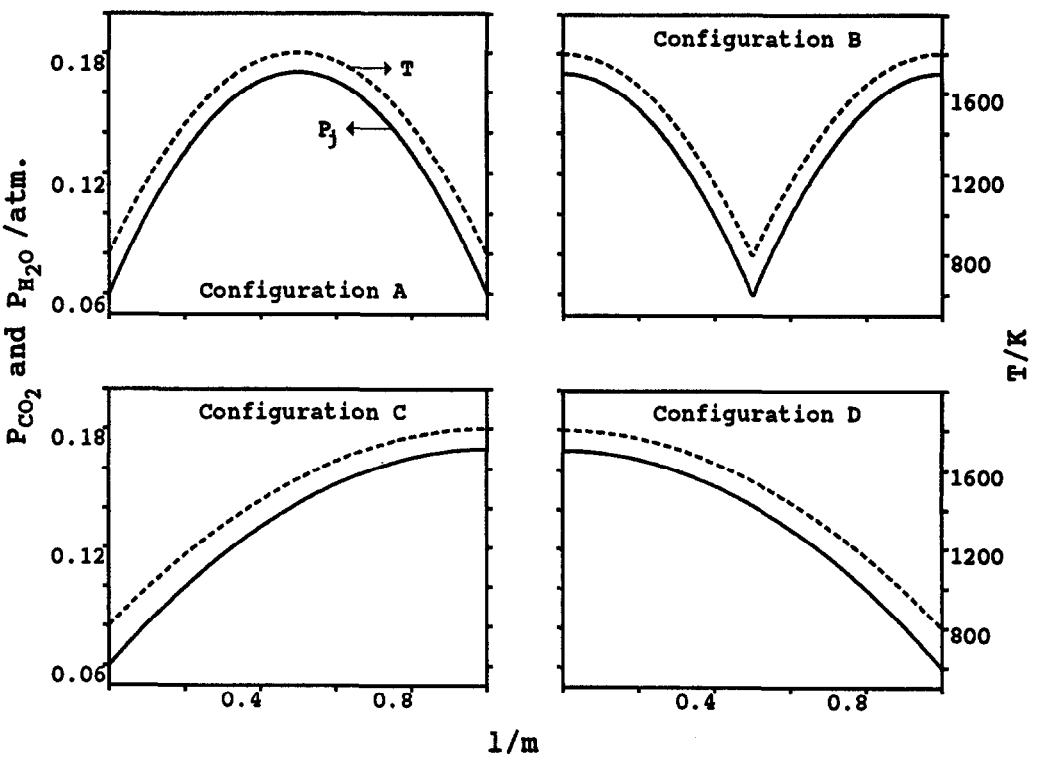

Fig. 2. Temperature and partial pressure profiles for four non-homogeneous paths.

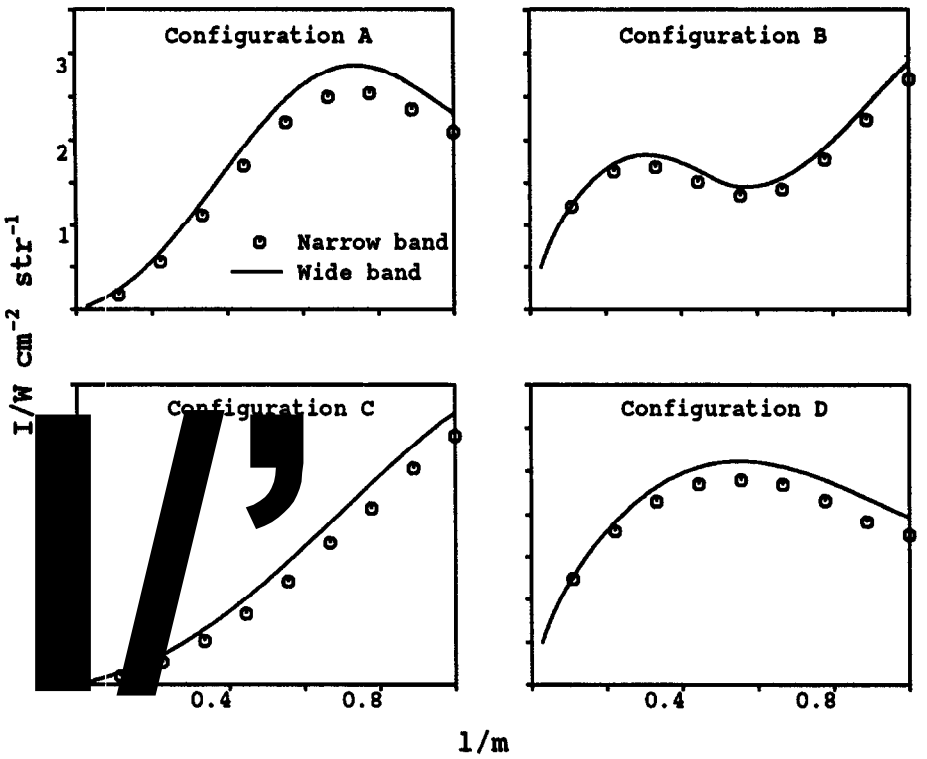

Fig. 3. Predictions of right-directed intensity for the four non-homogeneous paths.

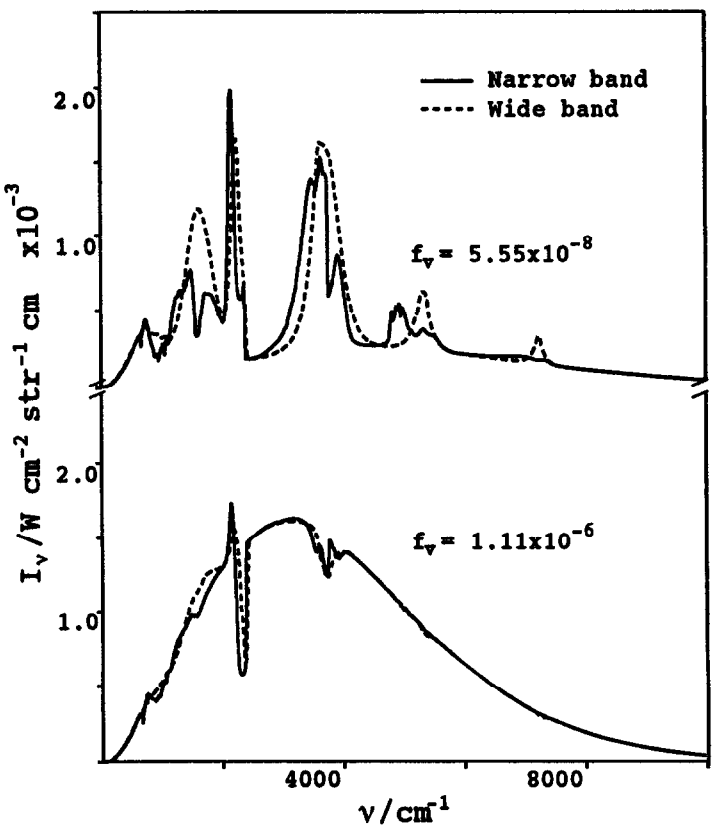

Fig. 4. Predictions of spectral intensity for low and high soot loadings.

loading case banded radiation due to gaseous species is seen to dominate the spectra, with the only serious discrepancy between the two approaches being the peak at $\nu \cong 1600$ cm^{-1} associated with the 6.3 μm band of H_2O. Despite this, and the slight overestimation of narrow band results by the wide band model at 5350 and 7250 cm^{-1} (corresponding to the 1.87 and 1.38 μm bands of H_2O) noticed by other authors [12, 18], the total integrated intensity predicted by the spectral method of 3.52 W cm^{-2} str^{-1} compares favourably with a value of 3.32 W cm^{-2} str^{-1} obtained from the narrow band approach. For high soot loadings soot emissions dominate the spectra, accounting for approximately 96% of the total intensity [19], although the major gas bands are still evident at low wave numbers where soot absorption is small. For this case the integrated intensities derived from the two models were within 2%.

Lastly, Grosshandler and Sawyer [20] did obtain measured emission spectra from experiments performed in a water-cooled furnace burning methanol, as well as temperatures and partial pressures of CO, CO_2 and H_2O along the line-of-sight used for the radiation measurements. Comparison between predictions of the spectral wide band approach and data obtained at an axial distance to furnace diameter ratio of three are given in Fig. 5. Overall, the wide band model tends to overestimate the peak intensities of the lower wave length bands of these species, and the 6.3 μm band of H_2O. The measured intensity distribution in the neighbourhood of the latter band is, in fact, typical of radiation that has traversed a hot gas layer followed by a cold layer. In such situations the radiation emitted by the hot gas is absorbed at the band centre, leaving the radiation in the wings of the band. The wide band model cannot predict this effect. Despite these problems, however, the total measured intensity of 1.02 W cm^{-2} str^{-1} does compare reasonably well with a value of 0.88 W cm^{-2} str^{-1} obtained from the wide band approach, and 0.84 Wcm^{-2} str^{-1} from the narrow band model.

4. MODEL APPLICATION

In the previous section the spectral wide band model was evaluated by comparing its predictions with experimental data and results derived from a statistical narrow band model for a number of homogeneous and non-homogeneous configurations. This allowed the performance of the model to be assessed, without the need for modelling of other physical and chemical processes clouding the issue. However, as one of the primary objectives of this work is the assessment of radiation models for use within a computational fluid dynamic framework, it is useful to consider the application of both techniques to predicting a real flame.

A laboratory scale jet flame studied by Faeth and co-workers [21–24] was selected for this exercise. These authors obtained detailed measurements of velocity, temperature and composition for a number of flames, as well as data on thermal radiation levels received at various positions about the flames. A turbulent non-premixed methane flame, stabilised on the rim of a 5 mm diameter pipe with a source Reynolds number of 11 700, is considered below.

4.1. *Description of jet flame structure model*

Predictions of the structure of this essentially parabolic flow were obtained by solving the axisymmetric forms of the appropriate Favre-averaged transport equations, with closure being achieved using a standard k–ε turbulence model. The gas-phase, non-premixed combustion process was modelled by assuming fast chemical reaction via the conserved scalar/prescribed probability density function (p.d.f.) approach using the laminar flamelet concept. A two-parameter, β-p.d.f. was used, with the form of this

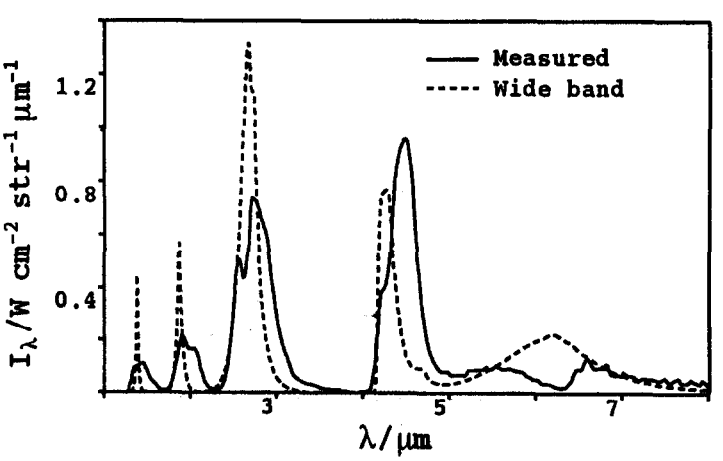

Fig. 5. Measured and predicted spectral intensity for a methanol furnace.

p.d.f. being specified in terms of the mean and variance of mixture fraction obtained from solution of modelled transport equations. Predictions of soot levels within the flame also incorporated through the solution of conservation equations for soot mass fraction and particle number density [1], although for the flame examined below soot levels were found to be sufficiently small to make no significant contribution to the emitted radiation field. The empirical constants which appear in the overall model described above were assigned standard values found to give acceptable agreement with experimental data in a wide range of flows [1, 25].

Laminar flamelet prescriptions were based on predictions of a detailed gas-phase chemistry scheme. Applications of this scheme to laminar counterflow diffusion flames burning methane were used to derive instantaneous relationships between mixture fraction and the density, temperature and composition of the combustion mixture. The results given below were derived from laminar calculations performed for an adiabatic flame with a strain rate of 15 s^{-1}, i.e. for an effectively unstrained flame. Radiative heat loss was accommodated by adjusting temperatures and densities derived from the adiabatic calculations in order to match turbulent flame predictions with the peak mean temperatures measured in the experiments.

Solution of the appropriate transport equations was achieved using a modified version of the GENMIX code [26]. In the absence of suitable experimental data, the fuel jet was assigned mean velocity and turbulence quantities typical of fully developed pipe flow. Numerical solutions were derived using expanding finite-volume meshes in both the axial and radial directions, with 3450×40 nodes in the x and r directions, respectively, being found sufficient to give predictions that were free of numerical error. Further details of the complete model may be found elsewhere [27].

The sensitivity of radiant emission to the temperature field, due to the non-linear dependence of the Planck distribution on temperature, makes its accurate prediction mandatory. Predicted mean temperatures were found to be in good agreement with experimental data [21–24], and generally within 15% of observed values, although there was a slight tendency to underpredict the radial extent of the jet. Predictions of the mean mass fraction of CO_2 were in similar agreement with available data, although for H_2O agreement was less satisfactory with the predicted peak mass fraction exceeding the measured value by approximately 40%. To assess the influence of differences between the predicted and observed jet flame structure on the radiation field, calculations of incident flux were obtained using the temperatures and species mass fractions predicted as above, and versions of the latter results that were scaled such that the jet width and peak species mass fractions matched the measured values. The relative difference between the two sets of incident fluxes was less than 10%. This analysis suggests that differences between the measured and predicted flow quantities of interest in any evaluation of models of radiative heat transfer can be expected to contribute an error of the order of 10% to predictions of incident flux—an acceptable level of inaccuracy given experimental uncertainties [22]. All the results given below were derived using the un-scaled flame structure results.

4.2. *Radiation model application*

In the results considered below the spectral wide band model was applied to predicting radiation intensities received from line-of-sight measurements taken along radial paths through the flame, and total fluxes received at various locations around the flame obtained using radiometers with a 150°, circular field of view. In making these predictions line-of-sight results were derived from radial temperatures and compositions obtained from the flame structure calculation, with the number of control volumes used to represent the non-homogeneous profiles through the flame being increased until received intensities were invariant to further refinement. Total fluxes were derived using an adaptation of the discrete transfer method [2, 28]. These computations again used temperatures and compositions derived from the structure calculation, with both the number of control volumes and rays required to determine received fluxes being increased until converged results were obtained.

All these predictions were made on the basis of Reynolds-averaged mean temperatures and Favre-averaged mean gaseous species mole fractions [1]. The actual intensity of radiation emitted from a fluctuating turbulent flame can, however, exceed values estimated using mean scalar properties since the physical parameters controlling radiative heat transfer interact in a highly non-linear fashion [29]. The influence of turbulence–radiation interactions was therefore ignored. The augmentation of radiative heat transfer by fluctuations of the temperature field does, however, depend crucially on the root mean square (rms) of the fluctuating temperatures [30]. Kritzstein and Soufiani [30] studied turbulence–radiation interaction in a homogeneous turbulent medium and demonstrated that for the configuration examined a relative rms temperature of 10% meant that the relative difference in band intensity calculated using the mean temperature and a stochastic simulation, which took the effects of turbulence fluctuations into account, was of the order of 8%. If the relative rms temperature was increased to 40%, then the difference in band intensity calculated by the two methods increased on average to 90%. No rms temperature measurements were made by Jeng *et al.* [21] for the jet flame considered below. Hassan *et al.* [31] did, however, obtain such measurements in a methane jet flame with a Reynolds number of 15000. For the latter flame, rms temperature of up to approximately 170 K occurred on the flame axis, at the same location as the peak mean temperature of 1700 K, and in other regions of the

flame the relative rms temperature had a peak value of 20%. It is therefore likely that turbulence–radiation interactions did not have a large effect on radiative heat transfer from the flame studied by Faeth and coworkers [21–24]. This is consistent with the findings of Jeng *et al.* [23, 24] whose predictions of spectral radiation intensities based on mean flame properties and a stochastic method differed by only 20%, with this difference being estimated to be comparable to uncertainties in the flame structure and radiation models used [24]. Spectral intensities derived using mean flame properties were also found to be in closest agreement with experimental data, with total radiative fluxes obtained on the same basis also being in close accord with measurements [23]. The neglect of turbulence–radiation interactions in the flame considered below therefore seems to be justified.

Figure 6 compares total intensities obtained using a radiometer pointing horizontally through the flame at three downstream locations. Predictions were made using both the spectral wide band and narrow band models, with the measurements being from Jeng *et al.* [24]. Similar comparisons for incident fluxes received about the flame are given in Fig. 7. The latter results were obtained [23] using a radiometer which was traversed in the radial direction, with its normal pointing vertically upwards, in the plane of the burner exit, and also parallel to the axis of the flame, and facing the axis, at a radial distance of 575 mm. Predictions of the spectral wide band model are seen to be in reasonable agreement with observed values of both integrated intensity and heat flux. This model does tend to overestimate incident flux data close to the base of the jet flame for radiometers traversed horizontally, but agreement with measured values is acceptable for radial distances greater than 150 mm. In addition, incident fluxes obtained as a function of vertical distance tend to be underpredicted for vertical heights above 700 mm. The results obtained are, however, comparable to those derived by Jeng *et al.* [23] using a narrow band approach, and slightly superior to predictions made using the narrow band model employed in the present study.

Overall, therefore, predictions of the spectral wide band model are in reasonable accord with observations, and comparable to results obtained using a narrow band approach. The superiority of predictions of the former model over those of the more accurate narrow band model must, of course, be considered to be to a large extent fortuitous—particularly in view of the proven accuracy of the latter approach—and largely due to inaccuracies in the flame structure calculation. When considering the usefulness of any model, however, both the physical error and the computational resource required must be assessed. For the predictions of total intensity and heat flux shown in Figs. 6 and 7, the narrow band model (with a wave number spacing of $\Delta\nu = 25$) required approximately nine times as much processor time as the spectral wide band model for no improvement in accuracy.

5. CONCLUSIONS

A spectral version of the exponential wide band model for calculating the radiation properties of molecular gases has been adapted for implementation within a computational fluid dynamic framework. Unlike the banded formulation of the same model, the spectral approach does not give rise to difficulties when trying to obtain coupled predictions of the radiation field from non-homogeneous combustion systems. Specifically, grey band assumptions are avoided, and as a consequence predictions of radiation intensity converge as the number of homogeneous elements used to represent a non-homogeneous profile increases, i.e. as the number of control

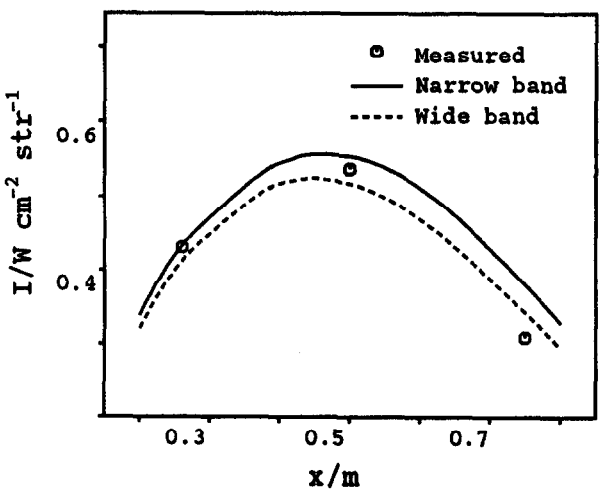

Fig. 6. Measured and predicted total intensities as a function of vertical distance.

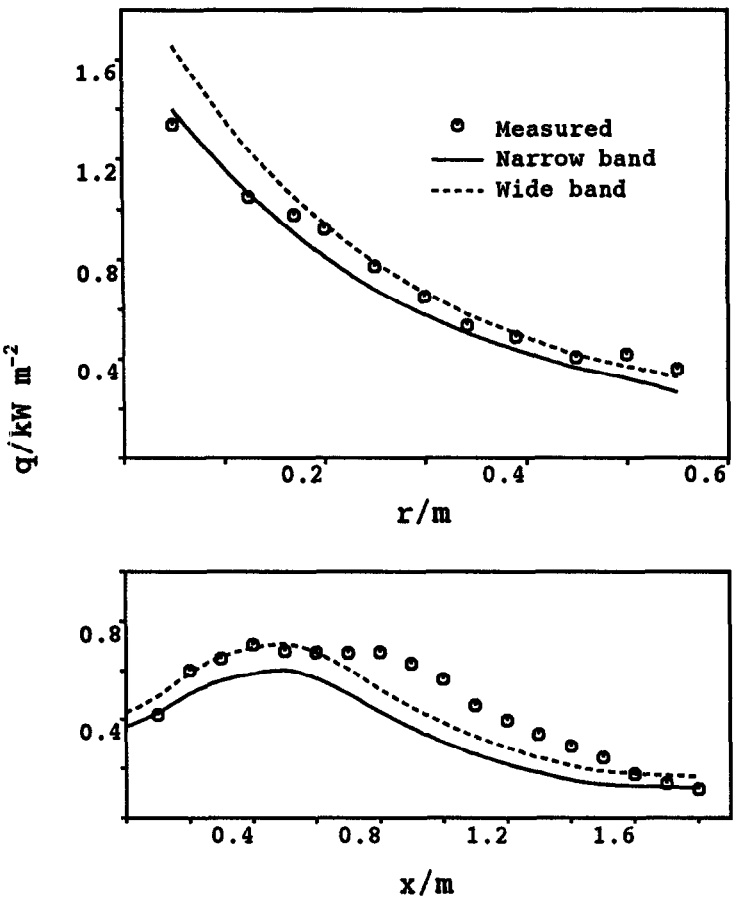

Fig. 7. Measured and predicted radiative heat fluxes incident on a line of horizontal and vertical receivers.

volumes used in any fluid dynamic calculation increases.

The spectral wide band model has been assessed by comparing predicted spectral and integrated quantities with experimental data and results derived from a statistical narrow band model for a number of idealised configurations. In addition, similar comparisons have been made for a laboratory scale non-premixed jet flame using coupled flame structure and radiative heat transfer calculations based on an adaptation of the discrete transfer method. Overall, the spectral wide band approach has been shown to be in reasonable agreement with experimental data, and to have an accuracy, for total quantities, comparable to that of the narrow band model whilst requiring almost an order of magnitude less computer processor time.

Acknowledgements—Helpful discussions with D. K. Cook and P. Docherty are gratefully acknowledged. This paper is published by permission of BG Technology.

REFERENCES

1. Fairweather, M., Jones, W. P. and Lindstedt, R. P., Predictions of radiative transfer from a turbulent reacting jet in a cross-wind. *Combust. Flame*, 1992, **89**, 45–62.
2. Lockwood, F. C. and Shah, N. G., A new radiation solution method for incorporation in general combustion prediction procedures. *Eighteenth Symposium (International) on Combustion*. The Combustion Institute, Pittsburgh, 1981, pp. 1405–1414.
3. Chandrasekhar, S., *Radiative Transfer*. Oxford University Press, London, 1950.
4. Edwards, D. K., Molecular gas band radiation. In *Advances in Heat Transfer*, Vol. 12, ed. T. F. Irvine Jr. and J. P. Hartnett. Academic Press, New York, 1976, pp. 115–193.
5. Hottel, H. C. and Sarofim, A. F., *Radiative Transfer*. McGraw-Hill, New York, 1967.
6. Grosshandler, W. L., Radiative heat transfer in nonhomogeneous gases: a simplified approach. *International Journal of Heat and Mass Transfer*, 1980, **23**, 1447–1459.
7. Edwards, D. K. and Balakrishnan, A., Thermal radiation by combustion gases. *International Journal of Heat and Mass Transfer*, 1973, **16**, 25–40.
8. Edwards, D. K. and Menard, W. A., Comparison of methods for correlation of total band absorption. *Appl. Optics*, 1964, **3**, 621–625.
9. Edwards, D. K., Glassen, L. K. Hauser, W. C. and Tuchscher, J. S., Radiation heat transfer in nonisothermal nongray gases. *Journal of Heat Transfer*, 1967, **89**, 219–229.
10. Weiner, M. M. and Edwards, D. K., Non-isothermal gas radiation in superposed vibration–rotation bands. *J. Quant. Spectrosc. Radiat. Transfer*, 1968, **8**, 1171–1183.
11. Komornicki, W. and Tomeczek, J., Modification of the

wide-band gas radiation model for flame calculation. *International Journal of Heat and Mass Transfer*, 1992, **35,** 1667–1672.
12. Docherty, P. and Fairweather, M., Predictions of radiative transfer from nonhomogeneous combustion products using the discrete transfer method. *Combust. Flame*, 1988, **71,** 79–87.
13. Modak, A. T., Radiation from products of combustion. *Fire Research*, 1978, **1,** 339–361.
14. Gerald, C. F. and Wheatley, P. O., *Applied Numerical Analysis*. Addison-Wesley, London, 1984.
15. Siegel, R. and Howell, J. R., *Thermal Radiation Heat Transfer*. McGraw-Hill, New York, 1972.
16. Grosshandler, W. L., Radiation from non-homogeneous fires. Technical Report RC79-BT-9, Factory Mutual Research, Norwood, 1979.
17. Ludwig, C. B., Malkmus, W., Reardon, J. E. and Thompson, J. A., Handbook of infra-red radiation from combustion gases. Technical Report, SP-3080, NASA, Washington, 1973.
18. Menguc, M. P. and Viskanta, R., An assessment of spectral radiative heat transfer predictions for a pulverized coal-fired furnace. *Proceedings of the 8th International Heat Transfer Conference*, Vol. 2, 1986, pp. 815–820.
19. Grosshandler, W. L. and Modak, A. T., Radiation from nonhomogeneous combustion products. *Eighteenth Symposium (International) on Combustion*. The Combustion Institute, Pittsburgh, 1981, pp. 601–609.
20. Grosshandler, W. L. and Sawyer, R. F., Radiation from a methanol furnace. *Journal of Heat Transfer*, 1978, **100,** 247–252.
21. Jeng, S.-M., Chen, L.-D. and Faeth, G. M., The structure of buoyant methane and propane diffusion flames. *Nineteenth Symposium (International) on Combustion*. The Combustion Institute, Pittsburgh, 1982, pp. 349–358.
22. Jeng, S.-M. and Faeth, G. M., Species concentrations and turbulence properties in buoyant methane diffusion flames. *Journal of Heat Transfer*, 1984, **106,** 721–727.
23. Jeng, S. M. and Faeth, G. M., Radiative heat fluxes near turbulent buoyant methane diffusion flames. *Journal of Heat Transfer*, 1984, **106,** 886–888.
24. Jeng, S.-M., Lai, M.-C. and Faeth, G. M., Nonluminous radiation in turbulent buoyant axisymmetric flames. *Combust. Sci. and Tech.*, 1984, **40,** 41–53.
25. Jones, W. P. and Whitelaw, J. H., Calculation methods for reacting turbulent flows: a review. *Combust. Flame*, 1982, **48,** 1–26.
26. Spalding, D. B., GENMIX: *A General Computer Program for Two-Dimensional Parabolic Phenomena*. Pergamon Press, Oxford, 1977.
27. Fairweather, M., Jones, W. P., Ledin, H. S. and Lindstedt, R. P., Predictions of soot formation in turbulent, non-premixed propane flames. *Twenty-fourth Symposium (International) on Combustion*. The Combustion Institute, Pittsburgh, 1992, pp. 1067–1074.
28. Cumber, P. S., Improvements to the discrete transfer method of calculating radiative heat transfer. *International Journal of Heat and Mass Transfer*, 1995, **38,** 2251–2258.
29. Cox, G., On radiant heat transfer from turbulent flames. *Combust. Sci. and Tech.*, 1977, **17,** 75–78.
30. Kritzstein, F. and Soufiani, A., Infrared gas radiation from a homogeneously turbulent medium. *International Journal of Heat and Mass Transfer*, 1993, **36,** 1749–1762.
31. Hassan, M. M. A., Lockwood, F. C. and Moneib, H. A., Fluctuating temperature and mean concentration measurements in a vertical turbulent free jet diffusion flame. *La Rivista dei Combustibili*, 1980, **38,** 357–372.